# Visual Anomaly Detection and Localization with a Patch-Wise Transformer and Convolutional Model

Afshin Dini[a] and Esa Rahtu[b]
*Unit of Computing Sciences, Tampere University, Finland*
*{firstname.lastname}@tuni.fi*

Keywords: Anomaly Detection, Anomaly Localization, Combined Transformer and Convolutional Networks.

Abstract: We present a one-class classification approach for detecting and locating anomalies in vision applications based on the combination of convolutional networks and transformers. This method utilizes a pre-trained model with four blocks of patch-wise transformer encoders and convolutional layers to extract patch embeddings from normal samples. The patch features from the third and fourth blocks of the model are then combined together to form the final representations, and then several multivariate Gaussian distributions are mapped on these normal embeddings accordingly. At the testing phase, irregularities are detected and located by setting a threshold on anomaly score and map defined by calculating the Mahalanobis distances between the patch embeddings of test samples and the related normal distributions. By evaluating the proposed method on the MVTec dataset, we find out that not only can this method detect anomalies properly due to the ability of the convolutional and transformer layers to present local and overall properties of an image, respectively, but also it is computationally efficient as it skips the training phase by using a pre-trained network as the feature extractor. These properties make our method a good candidate for detecting and locating irregularities in real-world industrial applications.



## 1 INTRODUCTION

Anomaly in vision applications refers to an image or area of an image that differs significantly from the normal behaviors of the majority of samples (Yang et al., 2021). Detecting and locating visual irregularities, which refer to the task of finding dissimilar samples and specifying the exact defective area of anomalous data (Chalapathy and Chawla, 2019), respectively, are active research topics in computer vision applications such as industrial inspections (Bergmann et al., 2019), video surveillance (Liu et al., 2018), and medical diagnosis applications (Fernando et al., 2021; Tschuchnig and Gadermayr, 2022).

In general, data-driven approaches like deep learning techniques are suitable candidates to deal with anomaly detection problems; however, they face some challenges due to the intrinsic properties of anomalies. Practically, irregularities rarely happen in real-world applications (Pang et al., 2021), and annotating anomalous samples for training a deep neural network is cumbersome in most cases. Moreover, irregularities are unknown before they occur (Chalapathy and Chawla, 2019). In other words, various types of anomalies in terms of shape, texture, color, and size can happen in real-world cases, and detecting unforeseen defects is difficult. Due to these reasons, most datasets such as MVTec (Bergmann et al., 2019) and BTAD (Mishra et al., 2021) utilized for evaluating anomaly detection problems only contain a few normal samples for training purposes which limits the selection and performance of the related deep learning approach.

Several semi-supervised approaches (Pang et al., 2021) that work properly with datasets containing only normal samples for the training phase have been developed recently to address the aforementioned challenges. Autoencoders (AEs) (Masci et al., 2011) and their extensions (Liu et al., 2020) are the most popular and simplest methods; however, they have difficulties in detecting subtle irregularities. Generative Adversarial Networks such GANomaly (Akcay et al., 2018) perform well in capturing semantic anomalies and are not appropriate for localizing irregularities in most cases (Di Mattia et al., 2019).

On the other hand, many researchers have focused on developing self-supervised approaches like Cut-

[a] https://orcid.org/0000-0001-6234-3322
[b] https://orcid.org/0000-0001-8767-0864



Dini, A. and Rahtu, E.
Visual Anomaly Detection and Localization with a Patch-Wise Transformer and Convolutional Model.
DOI: 10.5220/0011669400003417
In *Proceedings of the 18th International Joint Conference on Computer Vision, Imaging and Computer Graphics Theory and Applications (VISIGRAPP 2023) - Volume 5: VISAPP*, pages 144-152
ISBN: 978-989-758-634-7; ISSN: 2184-4321

Paste (Li et al., 2021) and CutOut (DeVries and Taylor, 2017), which attempt to train a network with normal and simulated anomalies. Although these methods can detect and locate different types of anomalies with various sizes properly, simulating anomalies might be cumbersome in the training phase.

Other semi-supervised methods such as VT-ADL (Mishra et al., 2021) try to utilize transformers in their architecture to improve their performance; however, large training datasets and powerful computational resources are required for training these models as they have a large number of trainable parameters (Yan et al., 2021).

In this work, we have proposed a new approach, inspired by (Defard et al., 2021), to address some of the aforementioned limitations. Our main goal is to develop a method that has high performance in anomaly detection and localization tasks while it is computationally efficient and can be trained with small datasets containing only a few normal samples. In this regard, we utilize a pre-trained network (Yan et al., 2021) containing several blocks of convolutional layers and patch-wise transformer encoders with skip connections as our backbone model to extract suitable representations of data. In the training phase, normal images are divided into patches with the same size as the patches used in transformer encoders, and fetched into the pre-trained model. The feature vectors from the last two blocks of the model are extracted and combined together to form the final representation of data. Then, the multivariate Gaussian distribution of each patch is found by calculating the mean and covariance of the related position in the combined feature vectors. At the testing phase, the Mahalanobis distance between the normal distribution and related feature vector of each patch is utilized to define the anomaly map. An upsampling and also Gaussian filtering is applied to the anomaly map to modify its size. Then, anomalies are detected based on assigning a threshold on the final anomaly map.

It is shown in section 4 that convolutional-transformer architecture can describe the overall and local properties of an image properly. Moreover, dividing images into patches of the same size as the ones used in the transformer encoders allows the model to be trained in such a way that it can detect fine-grained anomalies appropriately. Besides, this model is computationally efficient in the training phase since a pre-trained network is used as the backbone model of the method, which makes it a suitable candidate for real-world applications. We have evaluated our method on the MVTec dataset (Bergmann et al., 2019) and compared the results with previous state-of-the-art methods in section 4.

# 2 RELATED WORKS

From one point of view (Mohammadi et al., 2021), anomaly detection methods can be classified into three main categories as supervised, semi-supervised and unsupervised approaches, based on the types the available samples in the training datasets. Supervised deep learning methods like (Mohammadi et al., 2021) can be used only in specific applications with datasets containing a significant amount of anomalous samples for training purposes (Kong et al., 2019). On the other hand, unsupervised approaches (Ouardini et al., 2019) do not require labeled data for training; however, they have problems detecting small anomalies in high-dimensional space (Mohammadi et al., 2021).

Semi-supervised approaches that only utilize normal samples for training the model are the most popular ones. These methods vary from reconstruction-based approaches to self-supervised, and one-class detectors (Pang et al., 2021). Reconstruction-based methods are divided into several categories such as Autoencoders (AEs) (Masci et al., 2011) like VT-ADL (Mishra et al., 2021), inpainting approaches like InTra (Pirnay and Chai, 2022), Generative Adversarial Networks (GANs) (Di Mattia et al., 2019) like AnoGAN (Schlegl et al., 2017). These models are trained in such a way that they can reconstruct only normal images from a latent space while irregularities cannot be recreated properly, as a result of which the difference between the original and the reconstructed images can be utilized for detecting anomalies. Although these methods are various and simple in structure, they have their own limitations. For example, GAN-based approaches are sometimes hard to stabilize (Di Mattia et al., 2019), and Autoencoders are not able to detect fine-grained anomalies in some applications where the difference between original and reconstructed images is not significant (Pang et al., 2021).

One-class classifiers such as FCDD (Liznerski et al., 2020), and PSVDD (Yi and Yoon, 2020) attempt to specify a decision boundary on the feature space of normal images and detect anomalous samples as they are outside this area. Although these methods perform well in detecting subtle irregularities, they have some scalability problems (Pang et al., 2021) as the related feature space dimension increases. Moreover, patch-wise one-class classifiers like PSVDD (Yi and Yoon, 2020) are also computationally heavy as they utilize patches of images in the training and testing phases.

Self-supervised approaches such as CutPaste (Li et al., 2021) are two-stage frameworks that train a model in the first stage, also known as the proxy task,

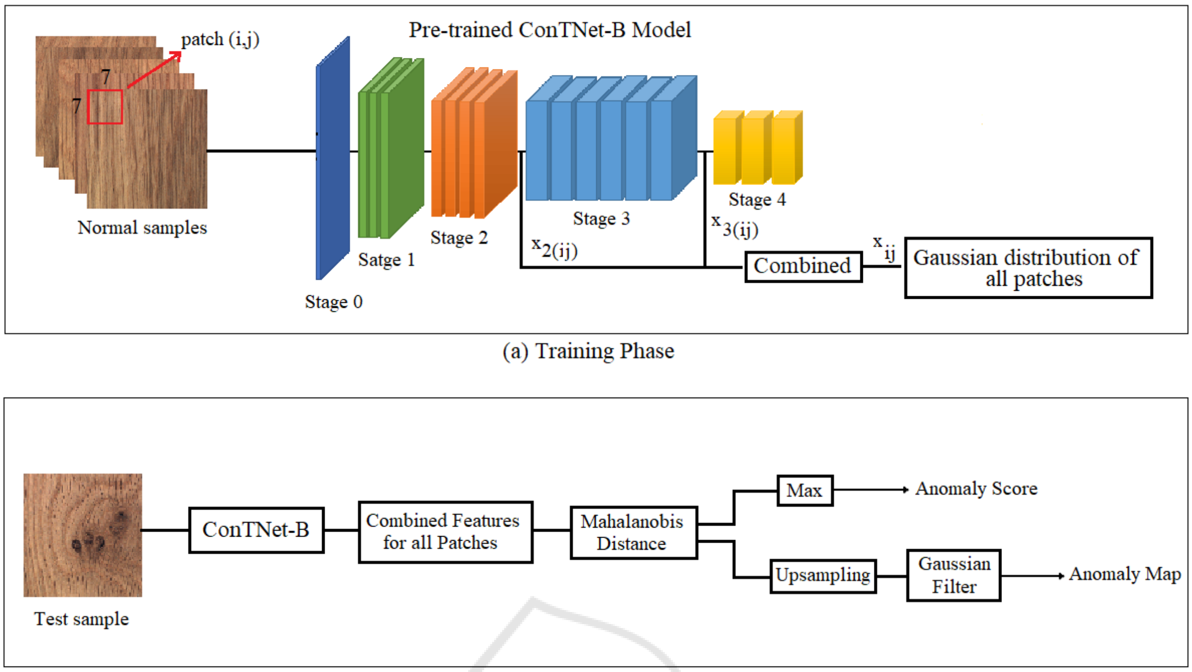


(a) Training Phase

(b) Testing Phase

Figure 1: Overview and model architecture of the proposed method for visual anomaly detection and localization. (a) A pre-trained ConTNet-B network is considered as the feature extractor in the training phase, and the Gaussian distributions of image patches are calculated based on the combined features. (b) Anomaly scores and maps are defined based on the Mahalanobis distance (Mahalanobis, 1936) calculated between normal and related test representations.

with normal samples and simulated anomalies created by applying different transformations on normal samples, and then utilize the trained model to extract features for the second stage which is the anomaly detection task (DeVries and Taylor, 2017). Although these methods are able to detect and locate defects appropriately, they are not generalized enough in some cases as they cannot simulate various types of unforeseen irregularities properly. Moreover, simulating anomalies can increase the computational costs of the training phase significantly based on the size of the network and the required number of anomalous samples (Li et al., 2021).

It is also good to mention that convolutional networks are used as the model architectures of most anomaly detection approaches. It is shown in (Yan et al., 2021) that although convolutional networks are good at describing the local features of an image, they are deficient in representing large receptive areas, as a result of which they restrict the performance of anomaly detection methods. On the other hand, transformer-based architectures can increase the performance of anomaly detection methods significantly as they can give suitable local and overall presentations of an image; however, they are much larger than convolutional networks, and more samples and computational resources are required for training them. Due to these reasons, only a few anomaly detection methods, such as VT-ADL (Mishra et al., 2021) and InTra (Pirnay and Chai, 2022) use transformers as their backbone models, and their performances are limited considering the fact that the number of training samples is limited to few hundreds in most anomaly detection datasets.

Our proposed method can address some of the aforementioned limitations while it leads to higher performance, as is discussed in more detail in section 3.

# 3 METHOD

## 3.1 Overview

We propose a method that attempts to extract the enriched patch features of normal samples utilizing a specific pre-trained network, ConTNet-B (Yan et al., 2021), and fit a multivariate Gaussian distribution on the combined embedding vector of each patch at the training step. Then, at the testing phase, the Mahalanobis distances (Mahalanobis, 1936) between the patch features of test samples and the related normal distributions are calculated and utilized for detecting and locating anomalies.

The overview and model architecture of the proposed method is described in detail in Fig.1. Selecting an architecture containing both convolutional and transformer encoders as a powerful feature extractor, dividing images into appropriate patches in the training stage in such a way that the model is able to extract enriched features, and combining specific middle layer features for anomaly detection task is the important properties of our method which we will discuss in detail in this section.

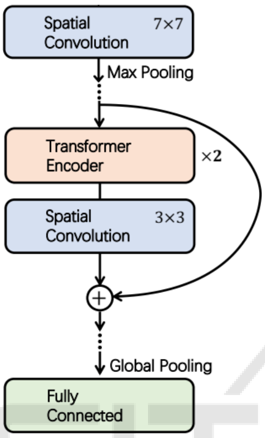


Figure 2: Illustration of ConT blocks, used in ConTNet-B model (Yan et al., 2021).

## 3.2 Model Architecture

One of the most important issues that can affect the performance of an anomaly detection method is the ability of the model to represent features for the detection task (Pang et al., 2021). If the feature embeddings can represent the semantic and local properties of the image properly, the anomaly detector would be able to identify the various types of subtle and large anomalies. It is shown that although convolutional networks are able to extract suitable local features of an image for anomaly detection problems (Bergman et al., 2020), they cannot represent large and semantic receptive areas appropriately in some cases (Yan et al., 2021).

On the other hand, transformers (Dosovitskiy et al., 2020) perform well in presenting overall features of data, as a result of which it seems that they can be utilized alongside the convolutional networks for extracting more detailed features; however, as we have tested several pre-trained convolutional-transformer-based architectures like CvT (Wu et al., 2021), CCT (Hassani et al., 2021), and ConViT (d'Ascoli et al., 2021) in our method in ablation study, we discover that they will not improve the performance of the anomaly detection method as they are not able to detect small anomalies in most cases. It seems that the convolutional layers in the combined models are not able to detect anomalies properly as it is supposed to be.

To solve this issue, we discover that using a convolutional-transformer-based architecture with patch-wise transformer encoders and skip connections between convolutional and transformer outputs (Yan et al., 2021) is a suitable candidate for our problem. We utilize the ConTNet-B model (Yan et al., 2021), pre-trained on ImageNet (Deng et al., 2009), as the feature extractor in our method, Fig.1(a). This model contains four stages, Tab.1, of several ConT blocks, Fig.2, containing convolutional layers and transformers. It is shown in section 4 that dividing the image into patches that match the patch-wise transformer encoders, in addition to the skip connections between outputs of transformers and convolutional layers, allows the model to represent more detailed embedding features for the detection problem.

Table 1: Illustration of ContNet-B model architecture in details (Yan et al., 2021).

| Stage | No. of blocks | Type |
|---|---|---|
| Stage 0 | 1 | CNN |
| Stage 1 | 3 | ConT |
| Stage 2 | 4 | ConT |
| Stage 3 | 6 | ConT |
| Stage 4 | 3 | ConT |
| Stage 5 | 1 | Average, FC |

Moreover, since ConTNet-B (Yan et al., 2021) has around 39.6 million trainable parameters, it is almost impossible to train this model from scratch using anomaly detection datasets like MVTec (Bergmann et al., 2019) that have only a few numbers of normal samples for training purposes. Even with data augmentation methods, training large networks like this model is cumbersome and requires a lot of computational resources, as a result of which we utilize the pre-trained model in our approach.

## 3.3 Patch Feature Extraction

We follow a similar patch feature extraction procedure in our method as SPADE (Cohen and Hoshen, 2020) and PaDiM (Defard et al., 2021), considering the fact that we select the patch size to match the patch-wise transformer encoders in the model architecture in order to extract detailed features from each patch. Therefore, an input image with size $W \times H$ is divided into square patches of size $P$. $P_{i,j}$ is the image patch at location $(i, j)$ where $(i, j) \in [1,W] \times [1,H]$.

The embedding vectors from the third and fourth stages of the model are extracted for each patch, $x_{2(ij)}$ and $x_{3(ij)}$, and combined together to form the final representation of each patch, $x_{(ij)}$, as is shown in Fig.1(a). The reason behind selecting the third and fourth embeddings is that not only it gives the best result amongst all possible combinations, as we experimentally find this, but also by considering the fact that deeper layers contain more detailed information than the shallower ones in deep models. The patch features are extracted and combined for all normal samples at all possible positions according to Eq.1 and utilized in the next step.

$$X_{ij} = \{x_{ij}^m : \quad (i,j) \in [1,W] \times [1,H],\ m \in [1,N]\} \quad (1)$$

where $X_{ij}$ is the set of patch features at position $(i,j)$ for all $N$ normal samples, and $x_{ij}^m$ is the combined feature vector of sample $m$ at position $(i,j)$.

### 3.4 Learning Normal Pattern

To learn the normal behavior of patches, we fit a multivariate Gaussian distribution, $\mathcal{N}(\mu_{ij}, \Sigma_{ij})$, on every set of image patches, $X_{ij}$, extracted from all normal samples at position $(i,j)$. $\mu_{ij}$ is the mean of all samples in $X_{ij}$ while the covariance, $\Sigma_{ij}$, is calculated according to Eq.2.

$$\Sigma_{ij} = \frac{1}{N-1} \sum_{m=1}^{N} (x_{ij}^m - \mu_{ij})(x_{ij}^m - \mu_{ij})^T + \varepsilon I \quad (2)$$

where $\varepsilon I$ is a small term to make sure that the covariance matrix is full rank and inversible as it is required for calculating the anomaly map and score.

Since the combined feature representations are created from embeddings of two middle layers, fitting the Gaussian distribution model on this embedding vector allows the model to capture various detailed information from different semantic levels, which can increase the performance of our method.

### 3.5 Anomaly Map and Score

In order to detect anomalous samples, a specific value, also known as anomaly score, should be assigned to each data sample, based on which we can identify defective samples by defining a threshold on these scores. Similarly, an anomaly map can be defined by assigning anomaly scores to pixels of an image according to which irregularities can be located in the related anomalous samples.

In order to define anomaly score and anomaly map, we follow the general approach (Rippel et al., 2021) and use Mahalanobis distance (Mahalanobis, 1936), Eq.3, to find the difference between patch features of test samples and their related normal distributions. This distance is considered as the anomaly score of all the pixels in the related patch.

$$M_{ij} = \sqrt{(x_{ij}^t - \mu_{ij})^T \Sigma_{ij}^{-1} (x_{ij}^t - \mu_{ij})} \quad (3)$$

where $M_{ij}$ and $x_{ij}^t$ are the anomaly map of the patch feature of the test sample at position $(i,j)$, respectively.

The calculated distance is assigned to all pixels of the related patch, and the maximum value will be considered as the anomaly score of the related test sample. The final anomaly map is created by upsampling the distance map to match the size of the original image and by applying a Gaussian filter to make it smoother.

By setting appropriate thresholds on anomaly scores and anomaly maps of all test samples, anomalies can be detected and located properly. We evaluated our method on the MVTec dataset (Bergmann et al., 2019) and discuss the results in section 4.

## 4 EXPERIMENT

### 4.1 Dataset and Metric

Following the common practice in the anomaly detection literature, we evaluate our approach on the MVTec dataset (Bergmann et al., 2019), which contains fifteen sub-datasets of high-resolution images from real-world industrial applications. This dataset comprises images with different sizes, types, colors, and textures which makes it a suitable candidate for assessing the performance and generalizability of the proposed method.

This dataset is made of five sub-datasets containing texture-type images and ten sub-datasets containing various object-type data samples. They comprise only a few normal images, varying from 60 to 391, for training a model, which seems to be a big challenge in developing deep models containing a huge number of trainable parameters. They also contain a few normal and anomalous test samples with defects of various sizes, shapes, colors, and types for testing the generalizability and performance of a method.

Moreover, images in this dataset have different resolutions varying from $700 \times 700$ to $1024 \times 1024$, which may be colorful or greyscale depending on the sub-dataset. This dataset also contains ground truth data, specifying the exact locations of anomalous areas in test samples according to which it can be used to assess the performance of the anomaly localization method.

Table 2: Comparison of our approach with patch-SVDD (Yi and Yoon, 2020), InTra (Pirnay and Chai, 2022), VT-ADL (Mishra et al., 2021), and CutPaste (Li et al., 2021) results in image-level anomaly detection on MVTec AD dataset (Bergmann et al., 2019), using AUROC metric.

| Category | | PSVDD | InTra | VT-ADL | CutPaste | Our Method |
|---|---|---|---|---|---|---|
| object | bottle | 98.6 | 100.0 | 94.9 | 98.3 | **100.0** |
| | cable | 90.3 | 70.3 | 77.6 | 80.6 | **99.4** |
| | capsule | 76.7 | 86.5 | 67.2 | **96.2** | 95.9 |
| | hazelnut | 92.0 | 95.7 | 89.7 | 97.3 | **100.0** |
| | metal nut | 94.0 | 96.9 | 72.6 | 99.3 | **99.8** |
| | pill | 86.1 | 90.2 | 70.5 | 92.4 | **95.6** |
| | screw | 81.3 | **95.7** | 92.8 | 86.3 | 92.2 |
| | toothbrush | 100 | **100.0** | 90.1 | 98.3 | 91.7 |
| | transistor | 91.5 | 95.8 | 79.6 | 95.5 | **99.8** |
| | zipper | 97.9 | 99.4 | 80.8 | **99.4** | 97.4 |
| | average | 90.8 | 93.0 | 81.6 | 94.3 | **97.2** |
| texture | carpet | 92.9 | 98.8 | 77.3 | 93.1 | **100.0** |
| | grid | 94.6 | **100.0** | 87.1 | 99.9 | 98.3 |
| | leather | 90.9 | 100.0 | 72.8 | 100.0 | **100.0** |
| | tile | 97.8 | 98.2 | 79.6 | 93.4 | **99.9** |
| | wood | 96.5 | 97.5 | 78.1 | 98.6 | **99.1** |
| | average | 94.5 | 98.9 | 79.0 | 97.0 | **99.4** |
| average | | 92.1 | 95.0 | 80.7 | 95.2 | **97.9** |



Table 3: Comparison of our approach with InTra (Pirnay and Chai, 2022), patch-SVDD (Yi and Yoon, 2020), CutPaste (Li et al., 2021), and PaDiM (Defard et al., 2021) methods in pixel-level anomaly detection on MVTec AD dataset (Bergmann et al., 2019), using AUROC metric.

| Category | | InTra | PSVDD | PaDiM | CutPaste | Our Method |
|---|---|---|---|---|---|---|
| object | bottle | 97.1 | **98.1** | 98.1 | 97.6 | 96.7 |
| | cable | 91.0 | 96.8 | 95.8 | 90.0 | **97.5** |
| | capsule | 97.7 | 95.8 | **98.3** | 97.4 | 97.4 |
| | hazelnut | **98.3** | 97.5 | 97.7 | 97.3 | 97.8 |
| | metal nut | 93.3 | **98.0** | 96.7 | 93.1 | 96.4 |
| | pill | **98.3** | 95.1 | 94.7 | 95.7 | 93.7 |
| | screw | **99.5** | 95.7 | 97.4 | 96.7 | 96.8 |
| | toothbrush | **98.9** | 98.1 | **98.7** | 98.1 | 97.6 |
| | transistor | 96.1 | 97.0 | 97.2 | 93.0 | **98.5** |
| | zipper | 99.2 | 95.1 | 98.2 | **99.3** | 96.2 |
| | average | 96.9 | 96.7 | **97.3** | 95.8 | 96.9 |
| texture | carpet | 99.2 | 92.6 | 98.9 | 98.3 | **99.3** |
| | grid | **98.8** | 96.2 | 94.9 | 97.5 | 96.5 |
| | leather | 99.5 | 97.4 | 99.1 | **99.5** | 98.6 |
| | tile | **94.4** | 91.4 | 91.2 | 90.5 | 93.4 |
| | wood | 88.7 | 90.8 | 93.6 | **95.5** | 92.9 |
| | average | 96.1 | 93.7 | 95.6 | **96.3** | 96.1 |
| average | | 96.6 | 95.7 | **96.7** | 96.0 | 96.6 |

Area Under the Receiver Operating Characteristic curve or AUROC is used to assess and compare the detection and the related localization performance of our method with the previous state-of-the-art results. In this regard, the anomaly detection ROC curve is created based on setting various thresholds on anomaly score, which is the maximum Mahalanobis distance of pixels of a test image as calculated in section 3.5. For the anomaly localization problem, the ROC curve is created based on setting thresholds on distance values of all patches of an image. In other words, for the localization problem, the true positive rate is plotted against the false positive rate at various threshold settings by considering the Mahalanobis distances of all pixels of test images from their related normal distributions.

## 4.2 Implementation Details

The ConTNet-B model (Yan et al., 2021), pre-trained on the ImageNet (Deng et al., 2009) is considered the feature extractor of our method. The images are resized to $224 \times 224$ at first and then divided into patches of size $7 \times 7$ in order to match the size of transformer encoders. It is good to mention that different patch sizes are tested in the ablation study; however, the best results are obtained with $7 \times 7$ patches as the larger patches cannot detect some small anomalies and smaller patches do not improve the performance and are sensitive to noises in few cases.

The extracted embeddings from the fourth layer are unfolded to match the size of the features from the third layer and then stacked together to form the final representations. Then, the calculated distance map is interpolated bilinearly in order to be the same size as the size of the original image, and a Gaussian filter with the variance of $\sigma = 4$ is applied to this map to form the final anomaly map. The maximum value of each anomaly map is considered as the anomaly score of the related test sample based on which, by setting an appropriate threshold, anomalous samples are specified.

## 4.3 Results

In order to assess the performance of our method and compare it with the results of previous methods, we run our approach on each sub-dataset and calculate the AUROC of each sub-dataset as well as the average AUROC for all texture-type and object-type sub-datasets.

The result of evaluating our method for the anomaly detection task is presented in Tab.2 and compared with the results of PSVDD (Yi and Yoon, 2020), InTra (Pirnay and Chai, 2022), VT-ADL (Mishra et al., 2021), and CutPaste (Li et al., 2021) methods. It is obvious that our method is able to detect anomalies precisely in the bottle, hazelnut, carpet, and leather sub-datasets. Moreover, the average AUROC is improved by 2.9 percent in object-type datasets, 0.5 percent in texture-types datasets, and 2.7 percent in all datasets, compared to the previous state-of-the-art results.

It is clear from Tab.2 that our method has a better performance by utilizing a feature-extractor with the combined convolutional and patch-wise transformer architecture compared to transformer-based methods such as InTra (Pirnay and Chai, 2022) and VT-ADL (Mishra et al., 2021), or convolutional-based model such as PSVDD (Yi and Yoon, 2020), and CutPaste (Li et al., 2021). Moreover, the computational cost of our method is much less than other patch-wise methods such as PSVDD (Yi and Yoon, 2020) since we take advantage of a pre-trained network instead of training the backbone model from scratch.

Our method also shows appropriate performance in the localization task since it defines the anomaly maps and anomaly scores at the same time from a pre-trained model without any additional effort for training a new model like what is implemented in CutPaste (Li et al., 2021) and PSVDD (Yi and Yoon, 2020). The result of evaluating our method for the anomaly localization task is presented in Tab.3 and compared to the previous methods.

It is shown that our method can locate defects in cable, transistor, and carpet sub-datasets better than previous methods and almost the same in other sub-datasets. For the anomaly localization problem, the average AUROC of our method is almost the same as InTra (Pirnay and Chai, 2022) and PaDiM (Defard et al., 2021) while it is improved by around one percent compared to other methods.

It is also important to notice that our method is able to locate the defective locations of an image properly in most cases, as it is shown in Fig.3; however, the results, presented in Tab.3, are based on the ability of the model to detect the correct number of anomalous pixels, as a result of which our method may get less AUROC in some datasets although the anomalous locations are detected properly. Various types of defects localization by our method for some texture and object-type samples are shown in Fig.3.

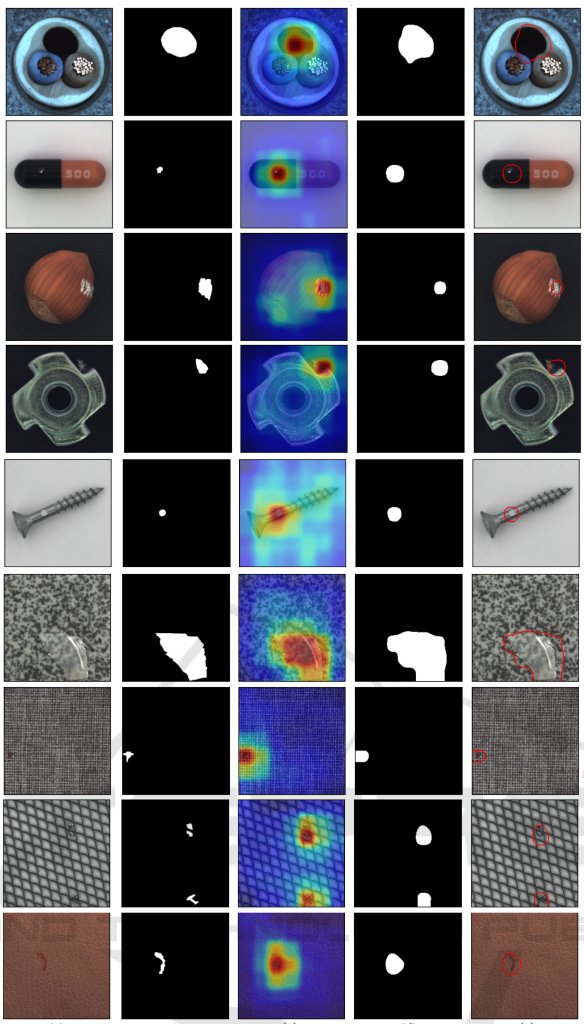


Figure 3: Visualization of defect localization using the proposed method. (a) Original image, (b) Ground truth map, (c) Predicted heat map, (d) Predicted map, (e) Predicted localization results.

## 5 CONCLUSION

We develop a new approach for detecting and locating anomalies in vision applications based on finding the Gaussian distribution of patch features of normal samples, extracted by a pre-trained patch-wise transformer and convolutional model which is able to present overall and local characteristics of samples precisely, and detecting anomalies based on the difference between these normal distributions and the related patch features in test samples.

We show that the proposed method has a superior ability to detect and locate different types and sizes of irregularities properly as we evaluate it on the MVTec dataset. Our method is also computationally efficient in the training phase as it skips the cumbersome training procedure of deep models from scratch, which makes it an appropriate approach to be used in real-world applications.

## REFERENCES

Akcay, S., Atapour-Abarghouei, A., and Breckon, T. P. (2018). Ganomaly: Semi-supervised anomaly detection via adversarial training. In *Asian conference on computer vision*, pages 622–637. Springer.

Bergman, L., Cohen, N., and Hoshen, Y. (2020). Deep nearest neighbor anomaly detection. *arXiv preprint arXiv:2002.10445*.

Bergmann, P., Fauser, M., Sattlegger, D., and Steger, C. (2019). Mvtec ad–a comprehensive real-world dataset for unsupervised anomaly detection. In *Proceedings* *of the IEEE/CVF conference on computer vision and pattern recognition*, pages 9592–9600.

Chalapathy, R. and Chawla, S. (2019). Deep learning for anomaly detection: A survey. *arXiv preprint arXiv:1901.03407*.

Cohen, N. and Hoshen, Y. (2020). Sub-image anomaly detection with deep pyramid correspondences. *arXiv preprint arXiv:2005.02357*.

d'Ascoli, S., Touvron, H., Leavitt, M. L., Morcos, A. S., Biroli, G., and Sagun, L. (2021). Convit: Improving vision transformers with soft convolutional inductive biases. In *International Conference on Machine Learning*, pages 2286–2296. PMLR.

Defard, T., Setkov, A., Loesch, A., and Audigier, R. (2021). Padim: a patch distribution modeling framework for anomaly detection and localization. In *International Conference on Pattern Recognition*, pages 475–489. Springer.

Deng, J., Dong, W., Socher, R., Li, L.-J., Li, K., and Fei-Fei, L. (2009). Imagenet: A large-scale hierarchical image database. In *2009 IEEE conference on computer vision and pattern recognition*, pages 248–255. Ieee.

DeVries, T. and Taylor, G. W. (2017). Improved regularization of convolutional neural networks with cutout. *arXiv preprint arXiv:1708.04552*.

Di Mattia, F., Galeone, P., De Simoni, M., and Ghelfi, E. (2019). A survey on gans for anomaly detection. *arXiv preprint arXiv:1906.11632*.

Dosovitskiy, A., Beyer, L., Kolesnikov, A., Weissenborn, D., Zhai, X., Unterthiner, T., Dehghani, M., Minderer, M., Heigold, G., Gelly, S., et al. (2020). An image is worth 16x16 words: Transformers for image recognition at scale. *arXiv preprint arXiv:2010.11929*.

Fernando, T., Gammulle, H., Denman, S., Sridharan, S., and Fookes, C. (2021). Deep learning for medical anomaly detection–a survey. *ACM Computing Surveys (CSUR)*, 54(7):1–37.

Hassani, A., Walton, S., Shah, N., Abuduweili, A., Li, J., and Shi, H. (2021). Escaping the big data paradigm with compact transformers. *arXiv preprint arXiv:2104.05704*.

Kong, Y., Huang, J., Huang, S., Wei, Z., and Wang, S. (2019). Learning spatiotemporal representations for human fall detection in surveillance video. *Journal of Visual Communication and Image Representation*, 59:215–230.

Li, C.-L., Sohn, K., Yoon, J., and Pfister, T. (2021). Cutpaste: Self-supervised learning for anomaly detection and localization. In *Proceedings of the IEEE/CVF Conference on Computer Vision and Pattern Recognition*, pages 9664–9674.

Liu, W., Li, R., Zheng, M., Karanam, S., Wu, Z., Bhanu, B., Radke, R. J., and Camps, O. (2020). Towards visually explaining variational autoencoders. In *Proceedings of the IEEE/CVF Conference on Computer Vision and Pattern Recognition*, pages 8642–8651.

Liu, Y., Li, C.-L., and Póczos, B. (2018). Classifier two sample test for video anomaly detections. In *BMVC*, page 71.

Liznerski, P., Ruff, L., Vandermeulen, R. A., Franks, B. J., Kloft, M., and Müller, K.-R. (2020). Explainable deep one-class classification. *arXiv preprint arXiv:2007.01760*.

Mahalanobis, P. C. (1936). On the generalized distance in statistics. National Institute of Science of India.

Masci, J., Meier, U., Cireşan, D., and Schmidhuber, J. (2011). Stacked convolutional auto-encoders for hierarchical feature extraction. In *International conference on artificial neural networks*, pages 52–59. Springer.

Mishra, P., Verk, R., Fornasier, D., Piciarelli, C., and Foresti, G. L. (2021). Vt-adl: A vision transformer network for image anomaly detection and localization. In *2021 IEEE 30th International Symposium on Industrial Electronics (ISIE)*, pages 01–06. IEEE.

Mohammadi, B., Fathy, M., and Sabokrou, M. (2021). Image/video deep anomaly detection: A survey. *arXiv preprint arXiv:2103.01739*.

Ouardini, K., Yang, H., Unnikrishnan, B., Romain, M., Garcin, C., Zenati, H., Campbell, J. P., Chiang, M. F., Kalpathy-Cramer, J., Chandrasekhar, V., et al. (2019). Towards practical unsupervised anomaly detection on retinal images. In *Domain Adaptation and Representation Transfer and Medical Image Learning with Less Labels and Imperfect Data*, pages 225–234. Springer.

Pang, G., Shen, C., Cao, L., and Hengel, A. V. D. (2021). Deep learning for anomaly detection: A review. *ACM Computing Surveys (CSUR)*, 54(2):1–38.

Pirnay, J. and Chai, K. (2022). Inpainting transformer for anomaly detection. In *International Conference on Image Analysis and Processing*, pages 394–406. Springer.

Rippel, O., Mertens, P., and Merhof, D. (2021). Modeling the distribution of normal data in pre-trained deep features for anomaly detection. In *2020 25th International Conference on Pattern Recognition (ICPR)*, pages 6726–6733. IEEE.

Schlegl, T., Seeböck, P., Waldstein, S. M., Schmidt-Erfurth, U., and Langs, G. (2017). Unsupervised anomaly detection with generative adversarial networks to guide marker discovery. In *International conference on information processing in medical imaging*, pages 146–157. Springer.

Tschuchnig, M. E. and Gadermayr, M. (2022). Anomaly detection in medical imaging-a mini review. *Data Science–Analytics and Applications*, pages 33–38.

Wu, H., Xiao, B., Codella, N., Liu, M., Dai, X., Yuan, L., and Zhang, L. (2021). Cvt: Introducing convolutions to vision transformers. In *Proceedings of the IEEE/CVF International Conference on Computer Vision*, pages 22–31.

Yan, H., Li, Z., Li, W., Wang, C., Wu, M., and Zhang, C. (2021). Contnet: Why not use convolution and transformer at the same time? *arXiv preprint arXiv:2104.13497*.

Yang, J., Xu, R., Qi, Z., and Shi, Y. (2021). Visual anomaly detection for images: A survey. *arXiv preprint arXiv:2109.13157*.

Yi, J. and Yoon, S. (2020). Patch svdd: Patch-level svdd for anomaly detection and segmentation. In *Proceedings of the Asian Conference on Computer Vision*.